Investigations into the Nature of a Silicoaluminophosphate with the Faujasite Structure

Ligia Sierra de Saldarriaga,† Carlos Saldarriaga, and Mark E. Davis*

Contribution from the Department of Chemical Engineering, Virginia Polytechnic Institute and State University, Blacksburg, Virginia 24061. *Received August 29, 1986*

Abstract: The physicochemical nature of a silicoaluminophosphate with the faujasite structure has been studied. The molecular sieve framework contains a homogeneous distribution of silicon, aluminum, and phosphorus and is negatively charged. Combustion in air of the charge-compensating organic cations produces hydroxyl groups which exhibit Brønsted acidity.

Several new classes of molecular sieves have recently been reported and include silicoaluminophosphates[1] (SAPO-*n*)[2] and metal-containing aluminophosphates (MeAPO-*n*[3a] and TAPO-*n*[3b]). These microporous solids not only exhibit properties characteristic of zeolites[4] and aluminophosphates[5] ($AlPO_4$-*n*) but also show unusual physicochemical traits ascribable to their unique chemical composition.

The new materials consist of tetrahedral oxide frameworks. For example, the SAPO molecular sieves contain tetrahedra of oxygen surrounded silicon, aluminum, and phosphorus arranged in a manner which can be considered as silicon substitution into a hypothetical $AlPO_4$-*n* framework. The silicon substitution can be for (1) aluminum, (2) phosphorus, or (3) an aluminum-phosphorus pair.[1b] Similar substitutions with titanium, cobalt, and other elements are postulated to occur in the formation of TAPO-*n* and MeAPO-*n* materials, respectively. Lok et al.[1b] report that mechanisms two and three are more likely than one for the SAPO materials since they exhibit cation exchange and they show an excess of aluminum over phosphorus.

To date, there is no conclusive evidence for the types of silicon substitution into the $AlPO_4$-*n* frameworks. Ito et al.[6] reported a crystal structure for the silicoaluminophosphate ZYT-6. However, the listed interatomic distances are not consistent[7] with the suggested silicon substitution. Appleyard et al.[8] performed solid-state NMR measurements for ^{27}Al, ^{31}P, and ^{29}Si on SAPO-5. Unfortunately, their sample contained very little silicon ($Si_{0.05}Al_{0.48}P_{0.47}$) leaving their conclusions speculative.

The purpose of our work is to investigate the nature of the silicon substitution into hypothetical aluminophosphate frameworks. Our study involves the SAPO materials rather than the TAPO or MeAPO solids since a larger knowledge base is available for solid-state ^{29}Si NMR compared to that for ^{59}Co or ^{47}Ti and that significant amounts of physicochemical data are readily available for zeolites. SAPO-37, the silicoaluminophosphate with faujasite structure,[1,2] will be investigated here because it contains a significant amount of silicon ($Si_{0.125}Al_{0.51}P_{0.365}$),[1] and it possesses the structure of the technologically important NaX, NaY, and ultrastable Y zeolites. Unfortunately, there is no aluminophosphate with faujasite structure which could be used for comparative purposes.

Experimental Section

a. Samples. The zeolites NaY[9] and TMA-faujasite[10] were synthesized by standard procedures. NH_4NaY was prepared by ion exchange of NaY with 1 N NH_4Cl. SAPO-37 was synthesized by a procedure similar to that of Lok et al. (example 43).[1a] Because of the precise synthesis procedure and the critical dependence of starting materials, we provide details of our method. Solution 1 was prepared by slowly adding 16.6 g pseudoboehmite alumina (Catapal-B) to a solution of 27.7 g of 85 wt % H_3PO_4 and 30.5 g of H_2O. The solution was extremely viscous and was stirred for approximately 7 h in order to obtain homogeneity. Solution 2 was prepared by adding 1.1 g of tetramethylammonium hydroxide pentahydrate ($TMAOH{\cdot}5H_2O$ obtained from Aldrich) to 116.0 g of 40 wt % tetrapropylammonium hydroxide (TPAOH obtained from Alfa). After the $TMAOH{\cdot}5H_2O$ dissolved, 3.1 g of fumed silica (Cab-O-Sil) were added to the solution. Solution 2 was not viscous and easily obtained homogeneity. Solution 2 was added slowly to solution 1, and the final mixture was stirred for approximately 20 h in order to achieve a homogeneous gel. Aging of this mixture at room temperature for 1-2 days slightly improved the yield of SAPO-37 which was obtained by heating the gel to 200 °C at autogeneous pressure for 24 h. The X-ray powder diffraction pattern and adsorption isotherms of SAPO-37 are comparable to those of NaY and therefore identify SAPO-37 as having the faujasite structure. The X-ray powder diffraction pattern of SAPO-37 was recorded and indexed on a Nicolet I2 automated diffraction system. The complete powder pattern indexed to cubic symmetry with $a = 24.612$ (4) Å by using lead nitrate as the internal standard.

b. NMR Measurements. Magic angle spinning ^{29}Si NMR spectra were recorded on a Nicolet NT-200 spectrometer. The field was lowered to 187.144 MHz giving a ^{29}Si frequency of 37.178 MHz with a spinning rate of 3.5 kHz. Conventional FT-NMR and cross-polarization, CP-NMR, ^{29}Si spectra were obtained, and the chemical shifts are reported relative to Me_4Si. FT-NMR and CP-NMR magic angle spinning ^{31}P spectra were recorded on a modified Nicolet NT-150 spectrometer with a ^{31}P frequency of 60.745 MHz and a spinning rate of 3-3.5 kHz. Chemical shifts are reported relative to 85 wt % H_3PO_4. Magic angle spinning ^{27}Al spectra were recorded on a modified Nicolet NT-360 spectrometer with an ^{27}Al frequency of 93.187 MHz. The spinning rate was varied between 8 and 11.3 kHz for identification of spinning side bands. The ^{27}Al chemical shifts are reported relative to sodium alum (within 1 ppm of $Al(NO_3)_3$ or $AlCl_3$). Magic angle spinning FT-NMR and CP-NMR ^{13}C spectra were recorded on a JEOL-FX200 spectrometer with a ^{13}C frequency of 50.309 MHz and a rotation rate of 3-4 kHz. Chemical shifts are reported relative to Me_4Si. The variable contact time experiments were performed on a modified Nicolet NT-150 spectrometer with a field of 37.5 MHz and a spinning frequency of 3.5-4 kHz.

c. Analysis. Infrared measurements were performed on an IBM IR/32 FTIR equipped with a Spectra-Tech Inc. diffuse reflectance cell which is coupled to a gas handling system. Calcination of samples SAPO-37 and NH_4NaY was performed in situ under flowing air at 600 °C for 2 h. Pyridine was injected in small amounts onto the samples after the temperature was lowered to 190 °C and the cell evacuated. Excess pyridine was pumped off at 190 °C prior to sampling.

Thermogravimetric analyses (TGA) and differential thermal analyses (DTA) were performed on a Dupont 950 thermogravimetric analyzer and 900 differential thermal analyzer, respectively.

Chemical analysis for carbon and nitrogen in SAPO-37 was performed by Galbraith Laboratories, Knoxville, TN. Silicon, aluminum, and

† Present address: Universidad de Antioquia, Departamento de Quimica, A. A. 1226, Medellin, Colombia.

(1) (a) Lok, B. M.; Messina, C. A.; Patton, R. L.; Gajek, R. T.; Cannan, T. R.; Flanigen, E. M. U.S. Patent 4440871, 1984. (b) Lok, B. M.; Messina, C. A.; Patton, R. L.; Gajek, R. T.; Cannan, T. R.; Flanigen, E. M. *J. Am. Chem. Soc.* **1984**, *106*, 6092-6093.
(2) The suffix "*n*" denotes a specific structure type as given in ref 1.
(3) (a) Wilson, S. T.; Flanigen, E. M. *Eur. Pat. Appl.* **1984**. (b) Lok, B. M.; Marcus, B. K.; Flanigen, E. M. *Eur. Pat. Appl.* **1984**.
(4) Breck, D. W. *Zeolite Molecular Sieves*; Wiley: New York, 1974.
(5) Wilson, S. T.; Lok, B. M.; Messina, C. A.; Cannan, T. R.; Flanigen, E. M. *J. Am. Chem. Soc.* **1982**, *104*, 1146-1147.
(6) Ito, M.; Shimoyama, Y.; Saito, Y.; Tsurita, Y.; Otake, M. *Acta Crystallogr., Sect. C: Cryst. Struct. Commun.* **1985**, *C41*, 1698-1700.
(7) Smith, J. V.; Bailey, S. W. *Acta Crystallogr.* **1963**, *16*, 801-811.
(8) Appleyard, I. P.; Harris, R. K.; Fitch, F. R. *Chem. Lett.* **1985**, 1747-1750.
(9) Breck, D. W. *Zeolite Molecular Sieves*; Wiley: New York, 1914; p 274.
(10) Barrer, R. M.; Denny, P. J.; Flanigen, E. M. U.S. Patent 3306922, 1967.

0002-7863/87/1509-2686$01.50/0

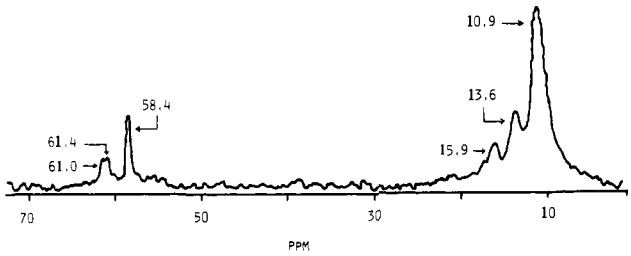

Figure 1. Cross-polarization ^{13}C NMR spectrum of SAPO-37.

phosphorus were analyzed by electron microprobe analysis by using an Applied Research Laboratories-SEMQ electron microprobe.

Results and Discussion

Chemical Compositions of SAPO-37. The chemical composition of SAPO-37 in terms of molar oxide ratios is

$$0.14TPA_2O{\cdot}0.05TMA_2O{\cdot}0.50SiO_2{\cdot}0.75P_2O_5{\cdot}Al_2O_3{\cdot}0.54H_2O$$

This composition is obtained from combining the chemical analysis for carbon and nitrogen with the water content determined by TGA/DTA (vide infra) and Si, Al, and P contents. These results compare favorably with those of Lok et al.[1] However, our material contains slightly more TPA_2O and P_2O_5 and less TMA_2O and H_2O. The ratio of TPA_2O/TMA_2O in the solid is 2.8 while that of the synthesis gel is 40. Thus, TMA is being concentrated in the solid. Attempts to synthesize SAPO-37 with lower TPA_2O/TMA_2O ratios failed to produce SAPO-37 but did crystallize SAPO-20 (silicoaluminophosphate with sodalite structure). Also, we have observed that TPA_2O/TMA_2O ratios above 40 tend to give SAPO-5. Thus, the gel phase TPA_2O/TMA_2O ratio is critical to the synthesis of SAPO-37.

The tetrahedral atom ratios are 4Al:3P:1Si to within experimental error. It appears from the bulk chemical analysis that Si^{4+} is substituting for P^{5+}. However, this is a global result and does not exclude the other substitution possibilities occurring at the local level. If a single negative charge accompanies the substitution of Si^{4+} for P^{5+} and all the organic cations are balancing the framework charge, approximately 75% of the overall charge is compensated by the organic cations while the remaining charge is balanced by hydronium ions.

The construction of the faujasite unit cell using the above composition reveals that there are 1.7 TPA molecules per supercage. This configuration leads to a fairly filled supercage. Since little room is available in the supercage, the TMA molecules are most probably located in the β-cages (vide infra). Each β-cage can contain no more than one TMA molecule. If all the TMA molecules are confined to the β-cages, they fill approximately two-thirds of the β-cages with the remaining third available to contain H_2O.

^{13}C NMR Results. Figure 1 shows the cross-polarization ^{13}C NMR spectrum of SAPO-37. The peak at 58.4 ppm is from TMA while all other peaks are from TPA. An impurity peak at 50 ppm (resonance not observed in other samples) is removed from the spectrum for clarity. Notice that the C_1-methylene peak of the TPA (carbon adjacent to the nitrogen) is split. Also, there are more than two peaks in the 20–5 ppm range which corresponds to the C_2-methylene and methyl carbons of the TPA. Thus, the TPA molecules exist in several environments. The broadness of these peaks suggest also that the TPA molecules have low symmetry.

Figure 2 gives the results of varying the contact time in the CP-NMR experiments. The peak at 58 ppm is from TMA while the broad peak around 10 ppm is from the methyl group of TPA. This figure illustrates that the TPA methyl signal appears at remarkably short contact time (signal detectable with contact times greater than 50 μs) and that there is no contact time that gives a quantitative spectrum. These results indicate that the TPA species are less mobile than the TMA molecules and/or have a superior proton source to that of TMA. Thus, the data illustrated in Figures 1 and 2 are consistent with the proposed configuration of the organic molecules.

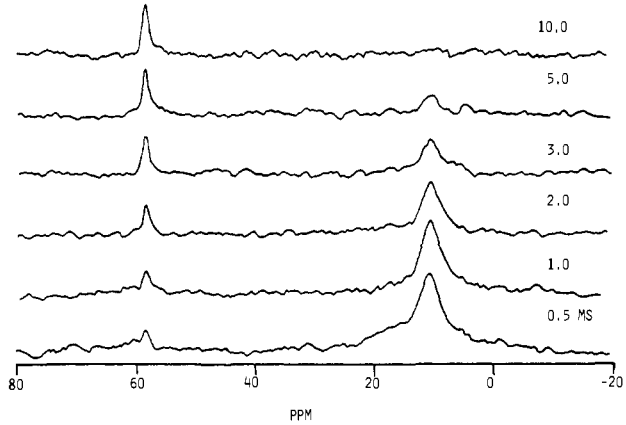

Figure 2. Effect of variable contact time in the cross-polarization ^{13}C NMR experiments of SAPO-37.

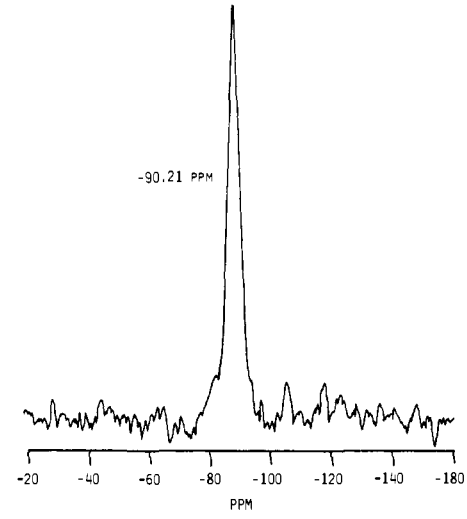

Figure 3. Cross-polarization ^{29}Si NMR spectrum of SAPO-37.

Table I. ^{29}Si Chemical Shift of Si(4Al) in Molecular Sieves

crystalline solid	Si/Al	δ (^{29}Si) from Me_4Si (ppm)	ref
NaY	2.5	-83.8	11
NaX	1.18	-84.6	11
NaA	1.0	-89.6	12
SAPO-5[c]	0.10,[a] (cannot be determined)[b]	-92.0	8
SAPO-37	0.25,[a] 1.0[b]	-90.21	this work

[a] Bulk composition. [b] Si/excess Al where excess Al = total aluminum - total phosphorus. [c] Speculated that silicon is Si(4Al).

^{29}Si and ^{31}P NMR Results. Figure 3 shows the CP ^{29}Si NMR spectrum of SAPO-37. The sample was not calcined. Only one peak at -90.21 ppm is observed. This signal is in the region that corresponds to silicon coordinated through oxygen atoms to 3, Si(3Al), or 4, Si(4Al), aluminum atoms.[11,12] Appleyard et al.[8] report a ^{29}Si chemical shift of -92 ppm for silicon in SAPO-5. Table I gives chemical shift data for Si(4Al) in zeolites and for the two SAPO materials. We list the SAPO-37 chemical shift as Si(4Al) for reasons given below. The -90 ppm shift is unusual for Si(4Al) in aluminosilicates, but there is precedence for such a shift in the case of zeolite A and N-A.[12] Also, if substitution mechanism 2 is dominant (observed from bulk composition), then silicon would be surrounded by four aluminum atoms. Mechanisms 1 and 3 require Si–O–P and Si–O–Si linkages, respectively. Appleyard et al.[8] observed a wide line width in their ^{29}Si signal

(11) Lippmaa, E.; Magi, M.; Samoson, A.; Tarmak, M.; Engelhardt, G. *J. Am. Chem. Soc.* **1984**, *103*, 4992–4996.
(12) Bennett, J. M.; Blackwell, C. S.; Cox, D. E. *Intrazeolite Chemistry*; The American Chemical Society: Washington, DC, 1983; pp 143–158.

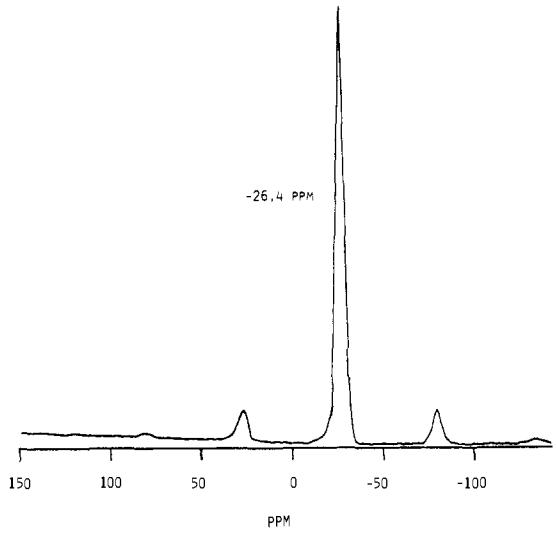

Figure 4. ^{31}P NMR spectrum of SAPO-37.

Table II. ^{31}P Chemical Shifts

molecular sieve	δ (^{31}P) from 85% H_3PO_4	ref
Pr_3-N-AlPO-5	-30.6	13
AlPO-5	-29.2	13
Et_4-N-AlPO-5	-28.6	14
AlPO-5	-27.8	14
AlPO-17	-24.2	14
AlPO-17 calcined	-29.9	14
AlPO-31	-30.2	14
AlPO-31 calcined	-29.6	14
Pr_3-N-SAPO-5	-28.4	8
SAPO-5	-29.6	8
SAPO-37	-26.4	this work

and could not overlook possibilities other than mechanism 2. For SAPO-37, there is a substantial amount of silicon present, and the resolution enhanced ^{29}Si spectra do not reveal structure in the -90 ppm peak. Thus, only one type of silicon environment is present in SAPO-37. If mechanism 3 occurs, then more than one silicon environment (Si(3Al) and Si(3P)) would be observed. Mechanism 1 yields Si(4P) environments which lead to positive framework charges. Thus, if mechanism 1 occurs, then so must mechanism 2 with the number density of (2) vastly exceeding that of (1) in order to give the overall chemical composition of the framework (vide supra). Simultaneous substitutions by mechanisms 1 and 2 would give two silicon environments which are not observed. However, there is no information available concerning the expected chemical shift for Si(4P). Table I shows also that the ratio of silicon to the aluminum in excess of the phosphorus content in SAPO-37 is 1.0. These results lead us to believe that silicon is in the single environment Si(4Al).

Figure 4 shows the FT ^{31}P NMR spectrum of SAPO-37 (not calcined). The single peak at -26.4 ppm is in good agreement with chemical shift values for tetrahedral phosphorus coordinated via oxygen to four aluminum atoms. Table II gives chemical shift values for P(4Al) in AlPO's and shows also the values obtained from the SAPO materials. The ^{31}P chemical shift for SAPO-5 is very similar to that of most of the AlPO's except for AlPO-17. The chemical shift for AlPO-17 is closer to that reported for SAPO-37. Recall that SAPO-5 contains very little silicon and is very "AlPO-like." Therefore, it is not surprising that the ^{31}P chemical shift from SAPO-5 is near that of the AlPO's. SAPO-37 contains a significant amount of silicon and is hydrophilic. Interestingly, AlPO-17 is the most hydrophilic AlPO listed in Table II.[14] It is possible that the chemical shift of ^{31}P in molecular sieves could be dependent upon the hydrophilic nature of the materials.

(13) Muller, D.; John, E.; Fahlke, B.; Ladwig, G.; Haubenreisser, U. *Zeolites* **1985**, *5*, 53-56.
(14) Blackwell, C. S.; Patton, R. L. *J. Phys. Chem.* **1984**, *88*, 6135-6139.

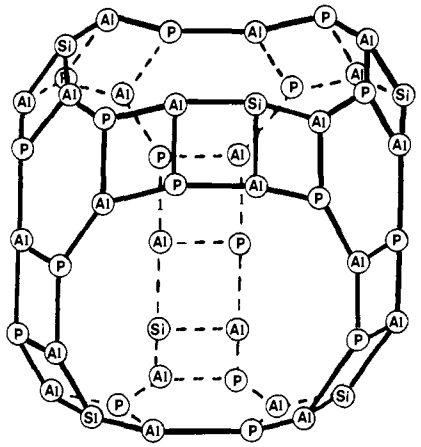

Figure 5. Model of SAPO-37 supercage. The lines represent oxygen atoms.

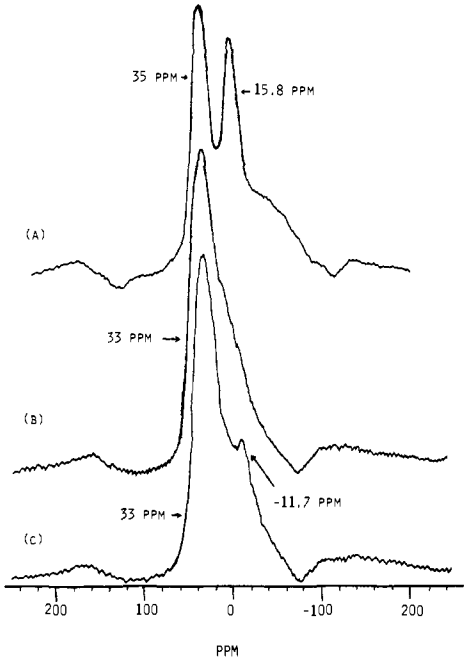

Figure 6. ^{27}Al NMR spectra of SAPO-37: (A) untreated, (B) calcined and partially rehydrated, (C) rehydrated (B).

However, when proton decoupling is performed in the ^{31}P NMR experiment with SAPO-37, there is only a slight narrowing of the peak. Therefore, most of the phosphorus in SAPO-37 is not close to protons.

The ^{31}P NMR data support further the conclusion that only substitution mechanism 2 is occurring in SAPO-37. This is because the ^{31}P NMR data show only a single peak which is assigned to P(4Al).

The ^{29}Si and ^{31}P NMR data show single chemical environments for Si and P. From this information, the bulk chemical composition, and the fact that the negative framework charges probably will be spatially distributed as far from one another as possible, we developed a model for the framework of SAPO-37. Figure 5 shows a representative supercage. This configuration is the only one we could derive which satisfies all the aforementioned criteria. In this model each silicon atom is coordinated via oxygen atoms to four aluminum atoms. Similarly each phosphorus atom is coordinated via oxygen atoms to four aluminum atoms. The fourth bond of each T-atom in Figure 5 which joins adjacent supercages is not shown for clarity. Interestingly, the model gives a single aluminum environment: aluminum coordinated via oxygen to three phosphorus and one silicon atoms.

^{27}Al NMR Results. Figure 6A illustrates the ^{27}Al NMR spectrum of SAPO-37 (not calcined). The figure shows two sharp peaks at 35 and 15.8 ppm and a broad peak around -20 ppm. The

broad peak is not a spinning side band since it appears at the same position in spectra recorded at different spinning rates. Normally the chemical shifts for tetrahedral and octahedral aluminum in zeolites are 65 to 51 ppm and 0 ppm, respectively. Tetrahedral and octahedral aluminum in aluminophosphates give chemical shifts of 41 to 29 ppm and −7 to −21 ppm, respectively. Thus, the ^{27}Al chemical shifts from SAPO-37 appear to be in the tetrahedral region of aluminophosphates and in the octahedral region of both. Figure 6B shows the ^{27}Al spectrum for calcined, partially rehydrated SAPO-37. Notice that only one broad peak occurs after calcination. The spectrum of untreated SAPO-37 can be interpreted as follows. Aluminum is quadrupolar, and second-order quadrupolar coupling has been observed in AlPO's.[14] We disregard second-order quadrupolar coupling as the source of the multiple peaks in spectrum (A) since only one peak appears after calcination. At least a portion of the TPA^+, TMA^+, and H_3O^+ (vide infra) are balancing the negative framework charge. The presence of guest molecules can produce different aluminum environments;[14] in the present case one environment has very low symmetry (broad signal). Upon calcination, these cations are removed to leave protons (vide infra). Thus, after calcination a single aluminum environment is observed as predicted by our model (Figure 5).

Figure 6C shows the ^{27}Al spectrum for calcined, rehydrated SAPO-37. In addition to the 33-ppm peak, a small peak at −11.7 ppm appears. This sample lost some crystallinity upon calcination and rehydration as observed by X-ray powder diffraction. The peak at −11.7 ppm is most probably due to extralattice aluminum from the partial destruction of the framework. We have noticed that the calcination of SAPO-37 is very moisture sensitive. Also, it is difficult to maintain complete crystallinity during this process. The line width of the 33-ppm peak decreases upon hydration. The broadening of the ^{27}Al resonance with dehydration has been observed in HY[15] and is attributed to enhanced distortion around aluminum. A similar effect could be occurring in SAPO-37.

Nature of Silicon Substitution. The previous data show conclusive evidence for silicon substitution into the hypothetical aluminophosphate framework by mechanism 2 alone. For SAPO-37, it appears that the substitution occurs in a uniform manner giving a regular distribution of silicon, aluminum, and phosphorus. It is most probably that pockets with zeolitic character, i.e., no phosphorus, do not occur because of the size of the charge balancing cations. The silicon to excess aluminum ratio is one for SAPO-37. Thus, a pocket of zeolitic material would require a relatively large number of balancing cations which could not be accompanied in the provided space. An example of this phenomenon is known. When sodalite is crystallized with TMA^+, the Si/Al ratio must increase in order to preserve electrical neutrality since only one TMA^+ molecule can reside in each β-cage.[16]

Thermal Decomposition Patterns. Figure 7 (parts A and B) shows the TGA and DTA results respectively for NaY, TMA–faujasite, and SAPO-37. NaY reveals the typical endotherm and weight loss caused by the removal of physically adsorbed water. TMA–faujasite shows three stages of weight loss: 25–200, 200–400, and 400–700 °C. These losses have distinct peaks in the DTA. The first loss is due to the desorption of water. The middle and final weight losses are accompanied by exotherms indicating that they are from the decomposition of the TMA. If the TMA–faujasite is cation exchanged with NaCl prior to the TGA/DTA experiments, the exotherm at 300–400 °C is removed. Therefore, the weight loss at 200–400 °C is from TMA located in the supercages. The final weight loss must be from TMA residing in the β-cages since it cannot be cation exchanged out of the β-cage. SAPO-37, like TMA-faujasite, shows three stages of weight loss. The first stage is from water desorption while the final stage is most probably due to removal of TMA from the

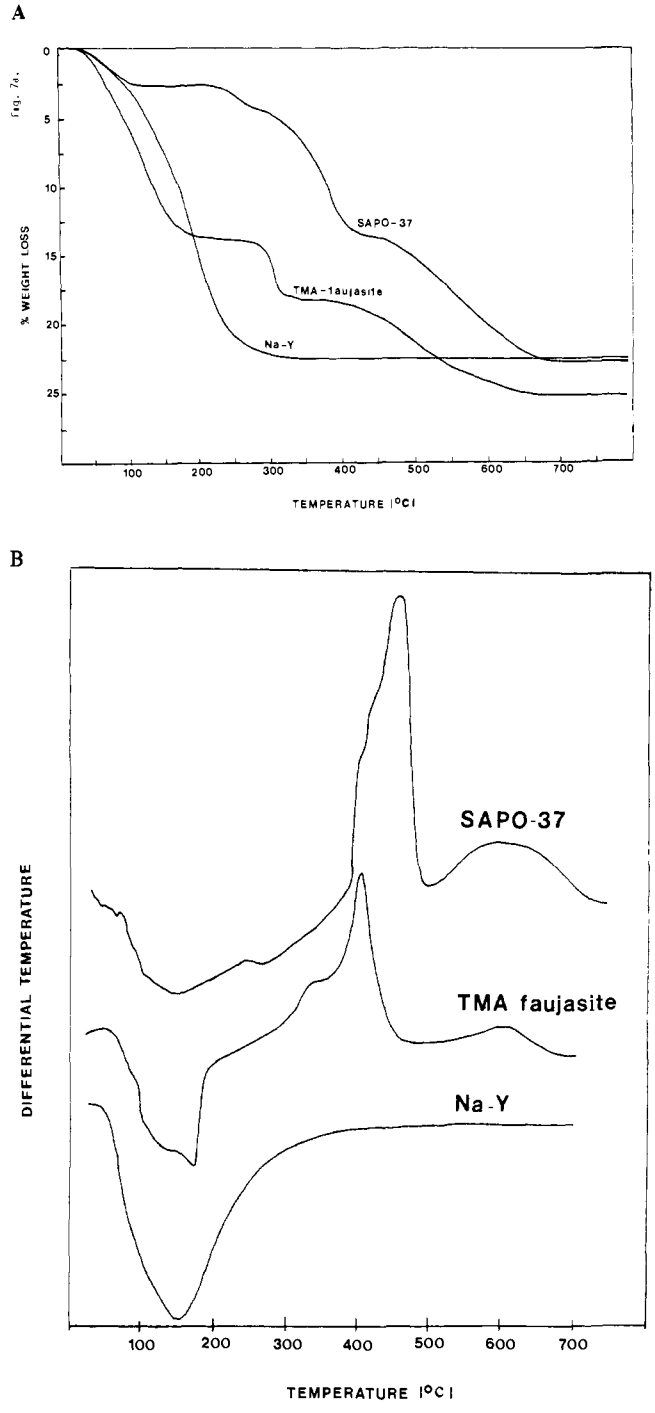

Figure 7. Thermal decomposition patterns for NaY, TMA–faujasite, and SAPO-37: (A) thermogravimetric analysis and (B) differential thermal analyses. All analyses were performed in air.

β-cages. The middle stage of weight loss is therefore due to the thermal decomposition of TPA in the supercage. These conclusions are further supported by the fact that if the TGA results are compared to the carbon and nitrogen analysis performed by independent procedures, the two sets of data correlate very well. These results are in complete agreement with our speculation of 1.7 TPA molecules per supercage and TMA residing only in β-cages.

Infrared Results. Figure 8 shows the infrared spectra of the structural region for NaY and SAPO-37. The zeolite NaY has a very characteristic spectrum.[17] Notice that the infrared spectra of SAPO-37 compare favorably to that of NaY again confirming

(15) Kentgens, A. P. M.; Scholle, K. F. M. G. J.; Veeman, W. S. *J. Phys. Chem.* **1983**, *87*, 4360–4361.
(16) Baerlocher, C.; Meier, W. M. *Helv. Chim. Acta.* **1969**, *52*, 1853–1860.
(17) Flanigen, E. M.; Khatami, H.; Szymanski, H. A. *Molecular Sieve Zeolites—I*; The American Chemical Society, Washington, DC, 1971; pp 201–228.

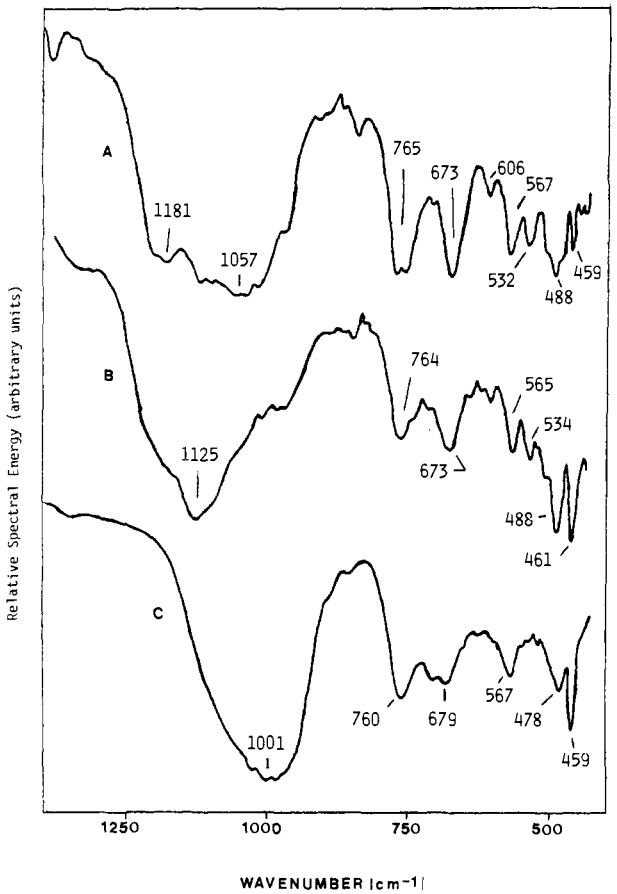

Figure 8. Infrared spectra of the structural region for NaY and SAPO-37: (A) untreated SAPO-37, (B) calcined SAPO-37, and (C) NaY.

the faujasite structure. The broad band around 1000 cm^{-1} for NaY has been assigned to the asymmetric stretching of tetrahedra[17] and is characteristic of many amorphous and crystalline materials. For SAPO-37, this region is shifted to higher wavenumbers and is changed slightly by calcination. The shift is due to the presence of phosphorus since the P–O bond distance is shorter than either Si–O or Al–O. The shorter bond distance of the P–O bond is also the reason SAPO-37 possesses a smaller unit cell compared to that of faujasite. The absorption at 567 cm^{-1} for NaY has been assigned to vibrations in the double six-membered rings. Notice that there are two absorptions in this region for SAPO-37 (565 and 535 cm^{-1}). The additional band in SAPO-37 must be due to the presence of phosphorus in the double six-membered rings. Other regions of the infrared spectrum which give absorptions from structure sensitive vibrations are 300–420 and 750–820 cm^{-1}. We do not have proper resolution in the lower wavenumber region to discern whether extra bands exist with SAPO-37. For the 750–820 cm^{-1} there is a lower wavenumber shoulder on the 764-cm^{-1} band, but the resolution is not adequate for assignment of a distinct band.

Figure 9 shows the infrared spectra of the hydroxyl region for SAPO-37 prior to and after calcination. Calcination of SAPO-37 generates absorption bands at 3737, 3629, 3567, and 3534 cm^{-1}. The nature of these hydroxyl groups can be deduced by comparing them with those developed from NH_4NaY calcination at similar conditions (see Figure 10C). The infrared bands in the hydroxyl group region for calcined NH_4NaY have been previously assigned[18,19] and are 3739 cm^{-1} (silanol), 3652 cm^{-1} (supercage), and 3541 cm^{-1} (β-cage). Thus, we assign the SAPO-37 hydroxyl groups bands as follows: 3737 cm^{-1} (silanol), 3629 cm^{-1} (supercage), and 3567–3534 cm^{-1} (β-cage).

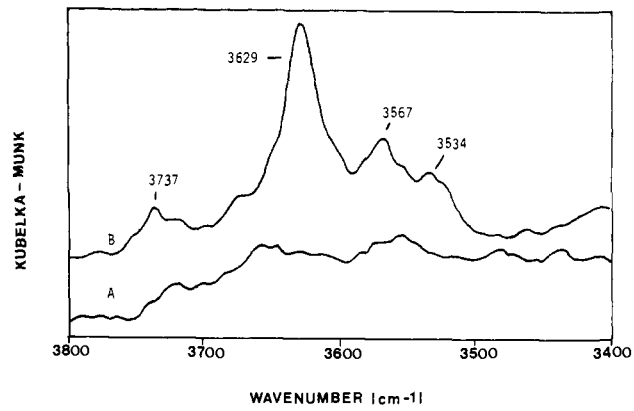

Figure 9. Infrared spectra of the hydroxyl region for SAPO-37: (A) untreated and (B) calcined.

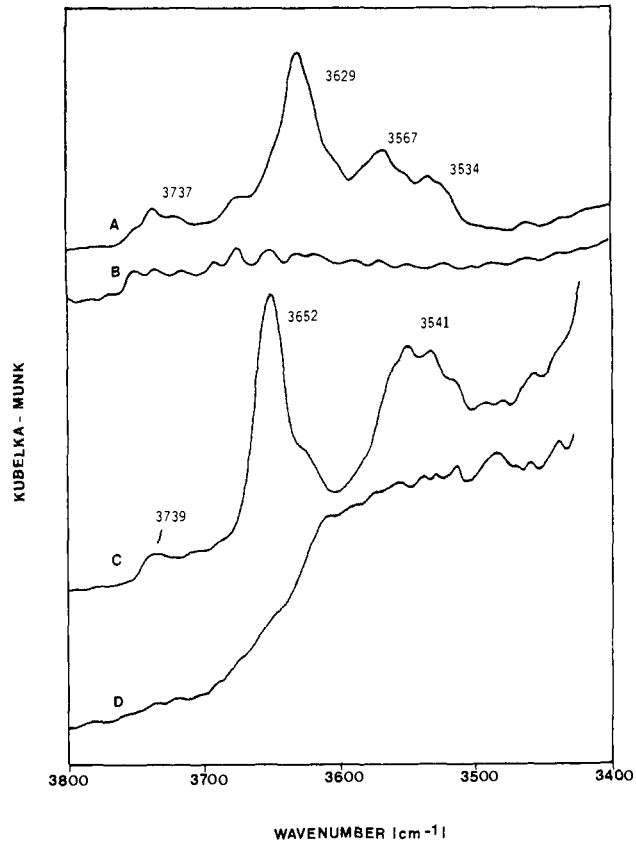

Figure 10. Effect of pyridine exposure on infrared spectra of the hydroxyl region for calcined SAPO-37 and NH_4NaY: (A) SAPO-37 before exposure, (B) SAPO-37 after exposure, (C) HNaY before exposure, and (D) HNaY after exposure.

Figure 10 gives the infrared spectra of the hydroxyl region for calcined SAPO-37 and NH_4NaY prior to and after exposure to pyridine. The results shown for NH_4NaY compare favorably to those reported previously.[19] Disappearance of the hydroxyl bands in SAPO-37 after exposure to pyridine indicates that the hydroxyl groups are Brønsted acids.

The generation of acid sites upon calcination of SAPO-37 indicates that the organic molecules are compensating framework charge.

Conclusions

The overall results of NMR and FTIR investigations of SAPO-37 lead to the following conclusions: 1. Silicon substitutes for phosphorus in the hypothetical aluminophosphate framework of faujasite structure. 2. There is a regular distribution of silicon, aluminum, and phosphorus in SAPO-37. 3. The organic cations are compensating the negative framework charge. 4. Calcination

(18) Kustov, L. M.; Bonovkov, V. Yu.; Kazansky, V. B. *J. Catal.* **1981**, *72*, 149–159.
(19) (a) Jacobs, P. A.; Uytterhoeven, J. B. *J. Catal.* **1972**, *26*, 175–190. (b) Jacobs, P. J.; Theng, B. K. G.; Uytterhoeven, J. B. *J. Catal.* **1972**, *26*, 191–201.

of SAPO-37 in air produces acidic hydroxyl groups.

Acknowledgment. Financial support of this work was provided by the National Science Foundation under the Presidential Young Investigator Award to M.E.D. Acknowledgment is made to the Colorado State University Regional NMR Center funded by the National Science Foundation Grant no. CHE 820-8821 for performing the solid-state NMR experiments. We thank Dr. Jan Wooten of Phillip Morris, Richmond, VA for performing some of the solid-state ^{13}C NMR experiments.

Registry No. TMAOH, 75-59-2; TPAOH, 4499-86-9.

Spectroscopic and Electrochemical Properties of Dimeric Ruthenium(II) Diimine Complexes and Determination of Their Excited State Redox Properties

Yael Fuchs, Sonita Lofters, Thomas Dieter, Wei Shi, Robert Morgan, Thomas C. Strekas,* Harry D. Gafney,* and A. David Baker*

Contribution from the Department of Chemistry, City University of New York, Queens College, Flushing, New York 11367. *Received June 9, 1986*

Abstract: The complexes $Ru(bpy)_2(ppz)^{2+}$ and $[(bpy)_2Ru(ppz)Ru(bpy)_2]^{4+}$, where ppz is the planar ligand 4′,7′-phenanthrolino-5′,6′:5,6-pyrazine, have been prepared and characterized. Resonance Raman spectra establish that the visible spectra of $Ru(bpy)_2L^{2+}$ and $[(bpy)_2Ru\text{-}L\text{-}Ru(bpy)_2]^{4+}$ complexes, where L is a bis-diimine, in general, are composed of MLCT transitions which terminate in the π^* orbitals localized on the different ligands. The luminescence, which is detectable at room temperature in fluid solutions of both the mono- and bimetallic complexes, can be assigned as a $L(\pi^*) \rightarrow Ru(II)$ t_2 transition. An approximate but general correlation between the lower energy MLCT absorption maximum and the emission maximum suggests that in many other bimetallic complexes of Ru(II) the emission energy is shifted beyond usual detection limits. Analysis of the emission and electrochemical data indicates that the MLCT states of bridged 2,3-dipyridylpyrazine (dpp) and ppz dimeric complexes are weak reductants but very strong oxidants. The implications of this general pattern of excited state redox potentials are discussed.

The luminescence from diimine complexes of Ru(II) has provided a unique probe of this transition metal's excited states.[1-3] Quantum yield and emission decay measurements provide access to the dynamics of intramolecular energy migration and dissipation. Quenching of the luminescent MLCT state offers, depending on the characteristics of the quencher, insights into the dynamics of intermolecular energy and electron transfer. Depending on the excited state potential (i.e., the difference in energy between the emissive state and the ground state oxidized and/or reduced states of the complex) as compared to that of the quencher, electron transfer may occur at a rate which may be predicted according to Marcus theory. However, electron transfer quenching studies of ruthenium(II) diimines provide evidence[1-3] of only one photon–one electron events. Since many important redox reactions involve multielectron transfer,[4,5] there is an interest in homogeneous and heterogeneous systems which convert multiple, photoinduced, single electron transfer events into subsequent multielectron transfer reactions. One such avenue of investigation involves polymeric Ru(II) complexes[6-14] which may be capable of acting as multielectron donors. Regardless of the kinetic constraints, which may be severe, the excited state redox potentials of such compounds are of pivotal significance in determining the photoinduced redox chemistry which may be available.

Monomeric ruthenium(II) diimine complexes exhibit intense MLCT transitions in the 400–600-nm region and corresponding emissions in the 600–700-nm region. Formation of the corresponding polymeric complexes results in the red shift of the lowest energy MLCT absorption band and the observation of a single red shifted emission. In each case, the red shift is associated with transitions involving the lowest energy π^* orbital of the bridging ligand. Although a number of bimetallic ruthenium(II) diimine complexes have been reported,[6-11] only one[6] has been found to be emissive in fluid solution at room temperature. Consequently, the excited state potentials of most bimetallic ruthenium(II) diimines, which determine their photoinduced redox chemistry, are not known.

Since subtle changes in coordination about Ru(II) can lead to a loss of luminescence, our strategy has focused on the design of bridging ligands which closely mimic the coordination of 2,2′-bipyridine at each Ru(II) center. To this end, the bridging ligand 2,3-di-2-pyridylpyrazine (dpp) was synthesized[6] and used to prepare $Ru(bpy)_2(dpp)^{2+}$ and $[(bpy)_2Ru(dpp)Ru(bpy)_2]^{4+}$. In

(1) Kalyanasundaram, K. *Coord. Chem. Rev.* **1982**, *46*, 159.
(2) Sutin, N.; Creutz, C. *Pure Appl. Chem.* **1980**, *52*, 2717.
(3) Watts, R. J. *J. Chem. Educ.* **1983**, *60*, 834.
(4) Meyer, T. J. *J. Electrochem. Soc.* **1984**, 221C.
(5) Ibers, J. A.; Holm, R. H. *Science* **1980**, *209*, 233.
(6) Braunstein, C. H.; Baker, A. D.; Strekas, T. C.; Gafney, H. D. *Inorg. Chem.* **1984**, *23*, 857.
(7) Rillema, D. P.; Mack, K. B. *Inorg. Chem.* **1982**, *21*, 3849.
(8) Rillema, D. P.; Callahan, R. W.; Mack, K. B. *Inorg. Chem.* **1982**, *21*, 2589.
(9) Dose, E.; Wilson, L. J. *Inorg. Chem.* **1978**, *17*, 2660.
(10) Hunziger, M.; Ludi, A. *J. Am. Chem. Soc.* **1977**, *99*, 7370.
(11) Haga, M.-A. *Inorg. Chim. Acta* **1980**, *45*, L183.
(12) Tinnemans, A. H. A.; Timmer, K.; Reinten, M.; Kraaijkamp, J. G.; Alberts, A. H.; van der Linden, J. G. M.; Schmitz, J. E. J.; Saaman, A. A. *Inorg. Chem.* **1981**, *20*, 3698.
(13) Curtis, J. C.; Bernstein, J. S.; Meyer, T. J. *Inorg. Chem.* **1985**, *24*, 385.
(14) Petersen, J. D.; Murphy, W. R., Jr.; Brewer, K. J.; Ruminski, K. R. *Coord. Chem. Rev.* **1985**, *64*, 261.

0002-7863/87/1509-2691$01.50/0